

Noise Analysis Method of Radiated EMI based on Non-linear Principal Component Analysis

Zhibo Zhu, Wei Yan, Yongan Wang, Yang Zhao*, Tao Zhang, and Junshuo Huang

School of Electrical and Automation Engineering
Nanjing Normal University, Nanjing, 210046, China
1822628862@qq.com, 61197@njnu.edu.cn, 544906768@qq.com, zhaoyang2@njnu.edu.cn*,
2901286136@qq.com, 13222755733@163.com

Abstract — Aiming at the radiated electromagnetic interference (EMI) noise of electronic equipment, a novel method of radiated EMI noise analysis based on non-linear principal component analysis (NLPCA) algorithm is proposed in this paper. In order to obtain multiple independent common-mode / differential-mode radiated sources, and to find the sources that cause the radiated noises that exceed the limit of standard, NLPCA algorithm is used to process the near-field radiated signals superimposed by multiple radiated sources. The simulation results show that NLPCA can successfully screen out the radiated EMI noises which exceed the limit of standard. Moreover, the experiments are carried out with three models: double-common-mode hybrid sources, double-differential-mode hybrid sources and common-differential-mode hybrid sources. Compared with the traditional independent component algorithm (ICA), the method proposed in this paper can separate the radiated EMI noise sources more accurately and quickly. It can be concluded that the accuracy of NLPCA algorithm is 10% higher than ICA algorithm. This work will contribute to trace the radiated EMI noise sources, and to provide the theoretical basis for the future suppression.

Index Terms — Mixed noise source, near-field noise analysis, NLPCA algorithm, noise separation, radiated EMI.

I. INTRODUCTION

With the rapid development of power electronic technology, the systems of modern electronic equipment are becoming more complex, and the electromagnetic waves generated by devices bring huge electromagnetic pollution to the environment [1-5]. In order to reduce the influence of radiated EMI noises, the most effective method is to suppress the noise source, therefore, the identification and diagnosis of electromagnetic radiated noise sources of electronic equipment have become the biggest challenge in EMI fault analysis [6-9].

At present, most scholars choose to study the

problem of radiated EMI noises from the perspective of electromagnetic field analysis. The electromagnetic radiated field of the loop antenna has been deduced by Moghaddam, and the interference effect of different radio frequency (RF) interference sources has been simulated finally [10-11]. A fast analysis method for spurious emission of RF circuits has been proposed by Hsieh and other scholars, which can quickly extract unnecessary radiated noises [12]. The near-far field conversion formula of antenna has been designed by Ricciardi, and the characteristics of the radiated target have been obtained by combing the near-field measurement [13]. Based on the transient emission time-domain model, radiated electromagnetic field analysis technology for the near-field has been proposed by Ravelo and others [14].

In addition, some scholars choose to analyze the radiated EMI noises from the perspective of signal analysis, and the signal analysis methods have been applied to diagnose of radiated EMI noises. The hybrid finite-difference time-domain analysis method for Maxwell's Equations has also been designed by Zhu and others [15]. An improved algorithm based on genetic algorithm has been applied to EMI problem analysis by Lin et al., which obviously saves working time [16]. Moreover, in order to evaluate the near-field and far-field EMI distribution of electromagnetic field, the full wave analysis method has been used by Arnaudov and other scholars [17]. Symmetrical component theory has been applied to model and analyze the characteristics of electromagnetic interference noise by Wang and others [18-20].

To solve and overcome the disadvantages of the traditional methods, a noise analysis method for radiated EMI of electronic equipment is proposed in this paper. The NLPCA is used to separate the near-field radiated time-domain signals, and to obtain multiple independent common-mode/ differential-mode radiated sources, so as to find out the sources that exceed the standard. Compared with the traditional ICA algorithm, the method can accurately and quickly find out the radiated EMI

noise sources, and is easier to operate and implement.

The outline of this paper is as follows. In Section II, the theoretical analysis of NLPCA algorithm is discussed. Section III studies the separation of the radiated EMI noise based on NLPCA. In Section IV, simulation of the radiated EMI noise based on NLPCA is carried out. In Section V, three groups of verification experiments are enforced. Section VI concludes the work.

II. THEORETICAL ANALYSIS OF NLPCA

A. Radiated EMI source

As shown in Fig. 1, there are many noise sources on the actual printed circuit board (PCB), and schematic diagram is shown in Fig. 2. There are n radiated sources, and the radiated noise generated by a single radiated source can be expressed as $E_1, E_2, E_3, \dots, E_n$, these radiations are superimposed to form the total radiated noises.

In this paper, the method for separating radiated EMI noise sources based on NLPCA algorithm is established. Firstly, the radiated noise signals on PCB are collected. Then the signals are separated by the NLPCA analysis. Finally, compared with the original signals on the PCB, several radiated noise sources that exceed the standard are screened out.

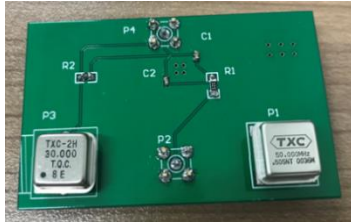


Fig. 1. The actual printed circuit board.

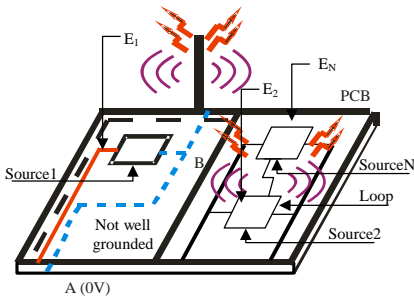


Fig. 2. Schematic diagram of space radiated EMI on PCB.

B. Principle of NLPCA

The NLPCA algorithm introduces the non-linear function into the standard principal component analysis (PCA) algorithm, so that the standard PCA algorithm can complete the separation of the source signals. Since the statistic of Gaussian data above the third order is zero,

the algorithm requires the input to be non-Gaussian data and needs to be pre-whitened at the same time.

The principle of the NLPCA algorithm includes the following three parts.

B.1. Mixed signal models

Blind signal separation refers to the process of recovering each independent component of the source signal only from the observed signal according to the statistical characteristics of the input signal. There are three main types of signals for blind signal separation research: linear mixed signals, non-linear mixed signals and convolutional mixed signals. In reality, due to the complexity of mixed system and the delay of signal propagation, the sensor usually obtains convolutional mixed signal.

The general model of convolutional mixed signal can be expressed as:

$$x(t) = A * s(t) = \sum_{p=-\infty}^{+\infty} A_p s(t-p), t = 1, 2, \dots, \quad (1)$$

$$s(t) = [s_1(t), \dots, s_n(t)]^T,$$

$$x(t) = [x_1(t), \dots, x_m(t)]^T,$$

where $s(t)$ is source signals with n mutually independence and identically distributed; $x(t)$ is m convolutional mixed signals; in this paper, $m=n$, A is the hybrid filter.

The purpose is to find a separation filter W_p such that $y(t)$ is an estimate of the source signal $s(t)$, as shown in formula (2):

$$y(t) = \sum_{p=-\infty}^{+\infty} W_p x(t-p) = [y_1(t), \dots, y_n(t)]^T, \quad (2)$$

where $y(t)$ is a n -dimensional column vector and W_p is a column of $n * n$ matrix, p is any real number.

The input and output systems in the z -transform domain can be expressed as:

$$X(z) = A(z)S(z),$$

$$Y(z) = W(z)X(z) = W(z)A(z)S(z) = C(z)S(z), \quad (3)$$

$$W(z) = \sum_{p=-\infty}^{\infty} W_p z^{-p}, A(z) = \sum_{p=-\infty}^{\infty} A_p z^{-p}, C(z) = W(z)A(z).$$

When $y(t)$ is an estimate of $s(t)$, there is:

$$C(z) = PD(z), \quad (4)$$

where P is an arbitrary permutation matrix, $D(z)$ is a non-singular diagonal matrix, its diagonal elements are:

$$c_i z^{-\Delta_i}, i = 1, \dots, n, \quad (5)$$

where c_i is a non-zero coefficient, and Δ_i is a real number.

B.2. Whitening algorithm

Signals need to be pre-whitened, which is conducive to speeding up the calculation speed of the algorithm. In this paper, based on the convolution hybrid structure, the whitening filter of convolutional mixed signals is obtained by defining the whitening criterion. Let the whitening filter $B(z)$ be:

$$B(z) = \sum_{\tau=-K}^K B_{\tau} z^{-\tau}. \quad (6)$$

Its adaptive algorithm is as follows:

$$v(t-K) = \sum_{\tau=-K}^K B_{\tau} x(t-K-\tau),$$

$$\Delta B_{\tau} = \alpha \left\{ B_{\tau} - \sum_{\tau'=-K}^K v(t-3K)v(t-3K-\tau+\tau')B_{\tau'} \right\}, \quad (7)$$

$$B\tau = \frac{1}{2}(B_{\tau} + B_{-\tau}^T),$$

where $\alpha(0 < \alpha < 1)$ is the iteration step size.

B.3. Recursive Least Square (RLS) algorithm

The cost function of convolution separation is:

$$\min J(W(t)) = \sum_{i=1}^t \beta^{t-i} \left\| v(i) - \sum_{p=0}^L W_p^T(t) f(y(i+p)) \right\|^2, \quad (8)$$

where v is the whitened signals of the mixed signals, and f is a non-linear function.

When the signals are sub-Gaussian signals, has:

$$f(y) = \tanh(y). \quad (9)$$

When the signals are super-Gaussian signals, has:

$$f(y) = y^3. \quad (10)$$

Use mapping approximation, we know that:

$$y(t) = \sum_{l=0}^L W_l(t)v(t-l) \approx \sum_{l=0}^L W_l(t-1)v(t-l). \quad (11)$$

The derivative of formula (8) with respect to $W_p(t)$:

$$\frac{\partial J(W(t))}{\partial W_p(t)} = -2 \sum_{i=1}^t \beta^{t-i} z(i+p)v^T(i)$$

$$+ 2 \sum_{i=1}^t \beta^{t-i} z(i+p) \sum_{p_1=0}^L Z^T(i+p_1)W_{p_1}(t). \quad (12)$$

Make formula (12) equal to zero, get the optimal matrix at time t :

$$W_p(t) = \left(\sum_{i=1}^t \beta^{t-i} z(i+p)z^T(i+p) \right)^{-1}, \quad (13)$$

$$\left(\sum_{i=1}^t \beta^{t-i} z(i+p)v^T(i) - z(i+p)zp(i) \right) = R^{-1}(t)C(t),$$

where

$$zp(i) = \sum_{\substack{p_1=0 \\ p_1 \neq p}}^L z(i+p_1)^T W_{p_1}(t),$$

$$R(t) = \sum_{i=1}^t \beta^{t-i} z(i+p)z^T(i+p), \quad (14)$$

$$C(t) = \sum_{i=1}^t \beta^{t-i} z(i+p)v^T(i) - z(i+p)zp(i).$$

From the point of view of filtering, formula (13) is a typical Weiner filter, so let $R(t) = P(t)$, has:

$$zp(t) = \sum_{\substack{p_1=0 \\ p_1 \neq p}}^L z(t+p_1)^T W_{p_1}(t-1). \quad (15)$$

From the matrix iterative inversion theorem and formula (16), an adaptive algorithm formula (17) for convolutional mixed blind source separation is obtained as follows:

$$R(t) = \beta R(t-1) + z(t+p)z^T(t+p), \quad (16)$$

$$C(t) = \beta C(t-1) + z(t+p)x(t) - z(t+p)zp(t),$$

$$W_p(t) = W_p(t-1) + [P(t)(z(t+p)v^T(t) - z(t+p)zp(t)) - Q(t)(z(t+p)z^T(t+p)W_p(t-1))]. \quad (17)$$

III. SEPARATION OF RADIATED EMI BASED ON NLPCA

In this paper, the NLPCA algorithm is applied to the separation of radiated EMI noise. Firstly, time-domain signals of radiated noises are collected by magnetic field probe through high-speed oscilloscope, the mixed signals are separated into multiple independent noise signals by the NLPCA algorithm, so as to screen out the sources of radiated EMI noises. The specific analysis flow chart is shown in Fig. 3.

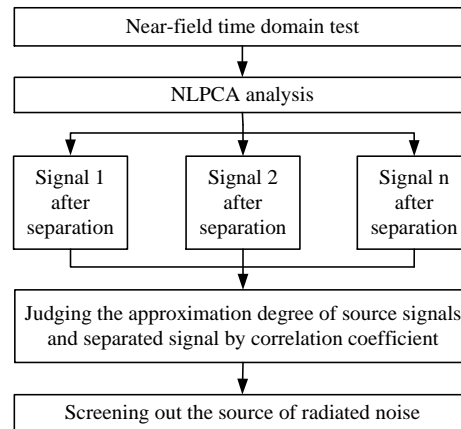


Fig. 3. Flow chart of radiated noise source screening.

A. Model of radiated EMI noises

In this section, a noise source model is established, as shown in Fig. 4. Radiated noises are generated between the three chips on the PCB through a cable. Use the near-field probe to measure the total radiated electric field at test points A, B, and C at the same time. It is worth noting that the highest test frequency of a high-speed digital oscilloscope should be greater than the frequency of the radiated electric field. During the test, the test distance, test angle, chip 1 cable, chip 2 cable and chip 3 cable were determined. The intensity of the radiated electric field at these three observation points can be expressed as:

$$E_A = E_{A1} + E_{A2} + E_{A3},$$

$$E_B = E_{B1} + E_{B2} + E_{B3}, \quad (18)$$

$$E_C = E_{C1} + E_{C2} + E_{C3},$$

where E_{A1} , E_{B1} , and E_{C1} are the radiated electric field generated by chip 1 at test points A, B, and C, respectively; E_{A2} , E_{B2} , and E_{C2} are the radiated electric fields generated by chip 2 at test points A, B, and C, respectively; E_{A3} , E_{B3} , and E_{C3} are the radiated electric fields generated by chip 3 at test points A, B, and C, respectively; the test distance and test angle are known.

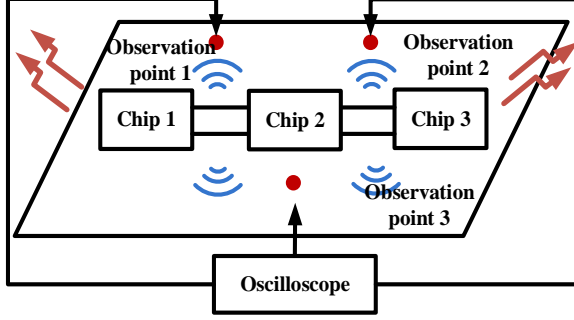


Fig. 4. Model of radiated EMI noise source.

Let,

$$K_{ij}(\tau) = \begin{pmatrix} K_{11}(\tau) & K_{12}(\tau) & K_{13}(\tau) \\ K_{21}(\tau) & K_{22}(\tau) & K_{23}(\tau) \\ K_{31}(\tau) & K_{32}(\tau) & K_{33}(\tau) \end{pmatrix}, \quad (19)$$

where $K_{ij}(\tau)$ is a n order filter with a delay of τ , n is the ratio of the cable length l to the wave speed v . $K_{ij}(\tau)$ represents the ratio of the radiated intensity to the current from the i th radiated source to the j th probe when the delay is τ .

Combined with formula (18) and formula (19), we can deduce that:

$$\begin{pmatrix} E_A(t) \\ E_B(t) \\ E_C(t) \end{pmatrix} = \sum_{\tau=0}^{l/v} K_{ij}(\tau) \begin{pmatrix} I_1^+(t-\tau) + I_1^-(t+\tau) \\ I_2^+(t-\tau) + I_2^-(t+\tau) \\ I_3^+(t-\tau) + I_3^-(t+\tau) \end{pmatrix}, \quad (20)$$

where $I_1(t)$, $I_2(t)$, and $I_3(t)$ are cable currents.

The electric field probe can output a voltage to the oscilloscope, which is proportional to the field strength. The scaling factor is called the antenna coefficient AF , which is:

$$AF = \frac{E}{V}. \quad (21)$$

In the test, the three electric field probes use the near-field electric field probe Stab 3 mm produced by Rohde & Schwarz, so the performance of the three probes is same, so the antenna coefficients are known and equal, that is $AF_1=AF_2=AF_3$. Therefore, the voltages can be obtained, as shown in formula (22):

$$\begin{pmatrix} V_1(t) \\ V_2(t) \\ V_3(t) \end{pmatrix} = \sum_{\tau=0}^{l/v} \frac{K_{ij}(\tau)}{AF_1 \cdot AF_2 \cdot AF_3} * \begin{pmatrix} I_1^+(t-\tau) + I_1^-(t+\tau) \\ I_2^+(t-\tau) + I_2^-(t+\tau) \\ I_3^+(t-\tau) + I_3^-(t+\tau) \end{pmatrix}. \quad (22)$$

B. Implementation steps of the radiated sources based on NLPCA algorithm

In this paper, the radiated EMI noises are separated by using the NLPCA algorithm, and the implementation steps are as follows.

Step 1: The radiated noise signals $s(t)$ are collected by testing, then the convolution signals $x(t)$ are obtained according to formula (1).

Step 2: Set the appropriate iteration step size, whitening filter $B(z)$ is designed.

Step 3: The cost function is obtained by formula (7), and then the derivative is zero to obtain the optimal matrix.

Step 4: Let $R(t) = P(t)$, then the separation filter $W_p(t)$ can be obtained from the matrix iterative inversion theorem and formula (16).

Step 5: Substitute the convolution signals $x(t)$ and the separation filter $W_p(t)$ into formula (2), the estimated signals $y(t)$ can be gained.

Step 6: In order to judge the performance index of the NLPCA algorithm, a similarity coefficient ζ is used to measure the approximate degree of the separated signals and the source signals:

$$\xi_{i,j} = \zeta(y_i, s_j) = \left| \sum_{t=1}^N y_i(t) s_j(t) \right| / \sqrt{\sum_{t=1}^N y_i^2(t) \sum_{t=1}^N s_j^2(t)}, \quad (23)$$

where N represents the number of sampling points.

The closer ζ is to 1, the better the separation effect is.

IV. SIMULATION OF RADIATED EMI BASED ON NLPCA

A. Basic performance simulation of NLPCA

Four independent source signals are created firstly, which are random signal, square wave signal, sine signal and cosine signal, and their waveforms are shown in Fig. 5 (a). Then, the four signals are mixed through a four order hybrid filter, the mixed signals are shown in Fig. 5 (b). Finally, the mixed signals are decomposed into independent four groups of signals according to the NLPCA algorithm, as shown in Fig. 5 (c).

The separation results in Fig. 5 (c) is compared with the source signals in Fig. 5 (a), it can be clearly seen that the mixed signals can be successfully separated into the source signals by the NLPCA algorithm, so the NLPCA algorithm can be applied to the mixed signals decomposition.

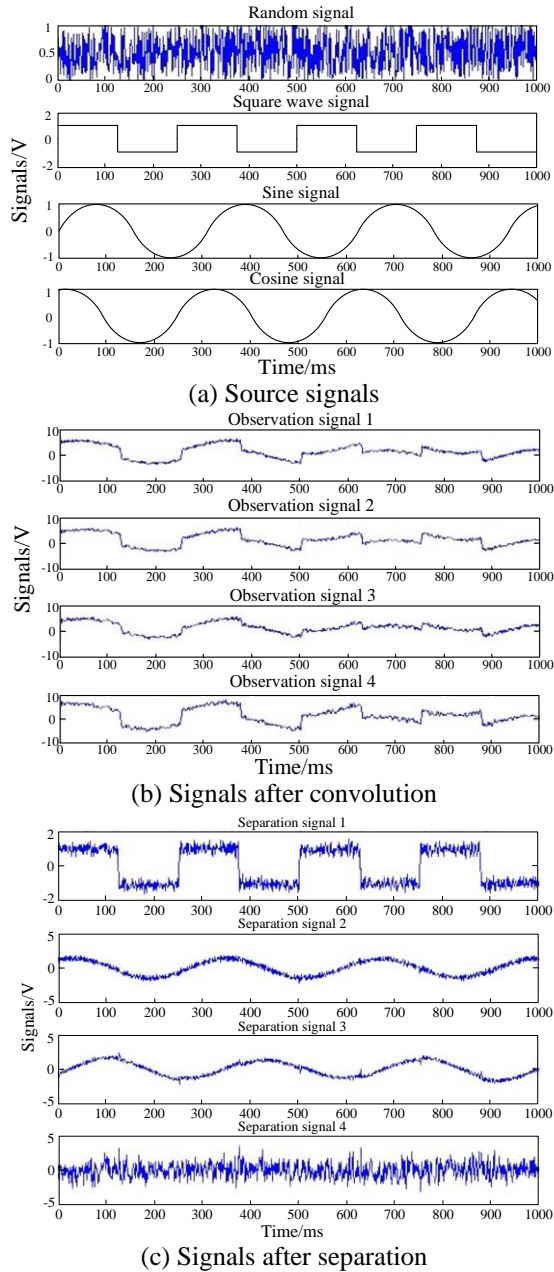


Fig. 5. NLPCA algorithm characteristic simulation.

B. Radiated EMI simulation of NLPCA

In order to verify the effectiveness of the NLPCA algorithm in electromagnetic compatibility, the method is applied to radiated EMI noises. As shown in Fig. 6 (a), these are two sets of independent differential-mode radiated noise sources. The two sets of mutually independent differential-mode signals are mixed by a random matrix according to NLPCA theory, and the mixing result is shown in Fig. 6 (b). After separation according to NLPCA algorithm, two sets of independent noise signals are obtained, as shown in Fig. 6 (c).

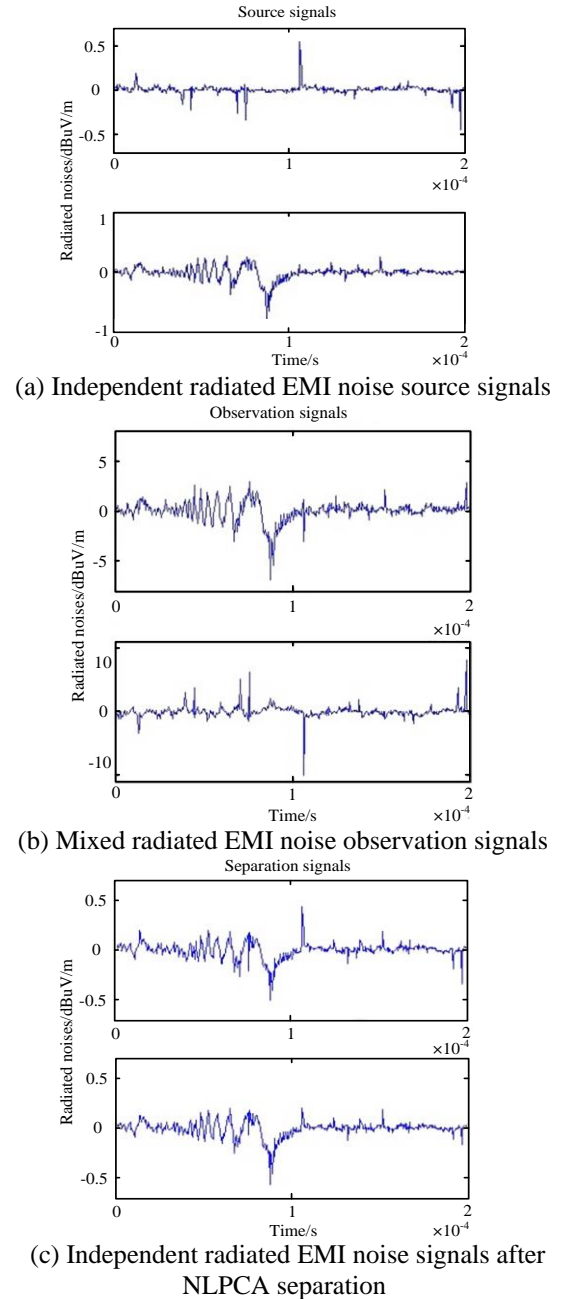


Fig. 6. Simulation results of radiated EMI noise sources based on NLPCA algorithm.

The separation results in Fig. 6 (c) is compared with the source signals in Fig. 6 (a), it can be seen that the NLPCA algorithm successfully separates two sets of mixed radiated differential-mode noises into two sets of independent differential-mode noises. Simulation results show that the algorithm can be successfully applied to EMI noise analysis.

In order to further verify the simulation results, according to formula (23) to calculate the correlation

between the accurately separated signal and the source signal, the correlation coefficients of the two differential-mode signals are 0.96 and 0.95, which shows that the separation results of NLPCA algorithm are ideal.

V. VERIFICATION EXPERIMENT OF RADIATED EMI BASED ON NLPCA

In this section, three different models are used to verify the feasibility of the NLPCA algorithm, which are the double-common-mode model, double-differential-mode model and common-differential-mode model.

In this experiment, multi-channel high-speed oscilloscope Tektronix DPO5204 (sampling rate is set to 1GS/s) and the near-field probe groups HZ-11 produced by R&S Company are used for testing. The testing diagrams are shown in Fig. 7.

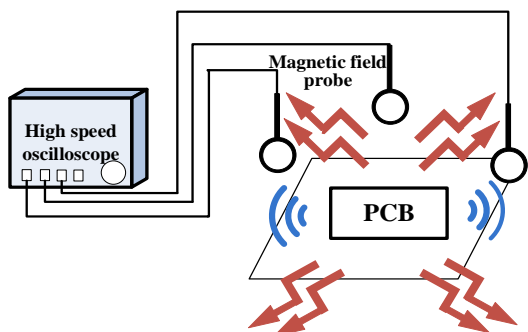


Fig. 7. Radiated EMI noises testing diagrams.

A. Double-common-mode model experiment

In the double-common-mode model experiment, the PCB contains two common-mode models, which are composed of two radiated sources of 30M crystal oscillator and 50M crystal oscillator. Two groups of mixed signals are measured through the double probes and the oscilloscope at the same time. Particularly, the probes are fixed through the clamp, and the distance between the double probes and the circuit is within 1 cm in this experiment. The white noises and the radiated EMI noises are shown in Fig. 8 (a) and Fig. 8 (b), respectively.

NLPCA analysis is performed on the measured mixed signals to obtain two independent signal noises, and the results are shown in Fig. 9. Compared with the time-domain signals collected, the similarity coefficients are 0.92 and 0.95, which are all close to 1, indicating that the NLPCA algorithm for noises separation are ideal.

B. Double-differential-mode model experiment

In the double-differential-mode model experiment, the PCB contains two differential-mode models, which are composed of two radiated sources of 30M crystal

oscillator and 50M crystal oscillator. Two groups of mixed signals are measured through the double probes and the oscilloscope at the same time. Particularly, the probes are fixed through the clamp, and the distance between the double probes and the circuit is within 1 cm in this experiment. The white noises and the radiated EMI noises are shown in Fig. 10 (a) and Fig. 10 (b), respectively.



(a) The white noises of double-common-mode model



(b) Radiated EMI noises of double-common-mode model

Fig. 8. Results of double-common-mode experiment.

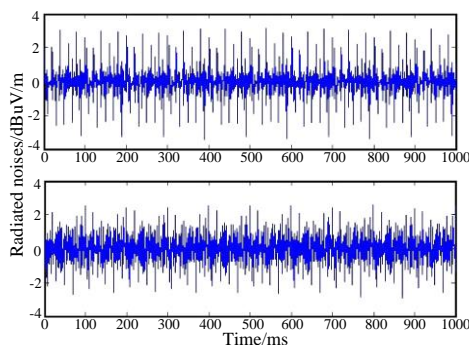


Fig. 9. Double-common-mode separation signals.



(a) The white noises of double-differential-mode model



(b) Radiated EMI noises of double-differential-mode model

Fig. 10. Results of double-differential-mode experiment.

NLPCA analysis is performed on the measured mixed signals to obtain two independent signal noises, and the results are shown in Fig. 11. Compared with the time-domain signals collected, the similarity coefficients are 0.93 and 0.96, which are all close to 1, indicating that the NLPCA algorithm for noises separation are ideal.

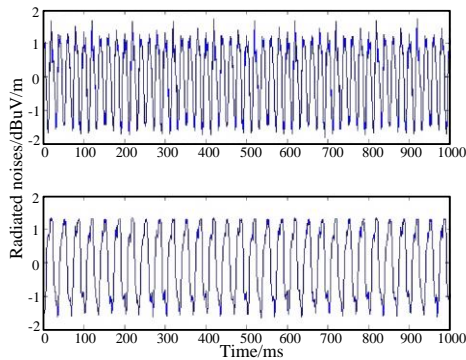


Fig. 11. Double-differential-mode separation signals.

C. Common-differential-mode model experiment

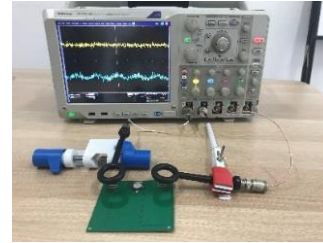
In the common-differential-mode model experiment, the PCB contains two common-difference-mode models, which are composed of two radiated sources of 30M crystal oscillator and 50M crystal oscillator. Two groups of mixed signals are measured through the double probes and the oscilloscope at the same time. Particularly, the probes are fixed through the clamp, and the distance between the double probes and the circuit is within 1 cm in this experiment. The white noises and the radiated EMI noises are shown in Fig. 12 (a) and Fig. 12 (b), respectively.

NLPCA analysis is performed on the measured mixed signals to obtain two independent signal noises, and the results are shown in Fig. 13. Compared with the time-domain signals collected, the similarity coefficients are 0.93 and 0.94, which are all close to 1, indicating that

the NLPCA algorithm for noises separation are ideal.



(a) The white noises of common-differential-mode model



(b) Radiated EMI noises of common-differential-mode model

Fig. 12. Results of common-differential-mode experiment.

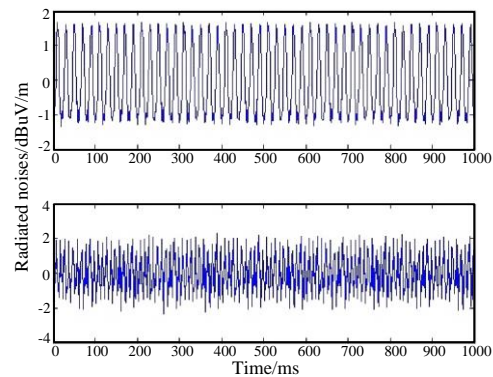


Fig. 13. Common-differential-mode separation signals.

Effectiveness of the separation of the radiated EMI noise signals based on the NLPCA algorithm is verified by the above three experiments. Compared with the ICA algorithm, NLPCA can separate the radiated EMI noise sources more accurately. The similarity coefficients of ICA and NLPCA of the three models are shown in Table 1. It can be concluded that the accuracy of NLPCA algorithm is 10% higher than ICA algorithm in separating radiated EMI noise signals. Moreover, on the basis of ICA, NLPCA introduces the fourth-order cumulant matrix of multivariate data, which has a wider application range and stronger universality.

Table 1: Similarity coefficients of three radiated EMI noise models

Radiated Source Model	Similarity Coefficient			
	ICA Algorithm		NLPCA Algorithm	
	First Noise	Second Noise	First Noise	Second Noise
Double-common-mode	0.81	0.83	0.92	0.95
Double-differential-mode	0.82	0.85	0.93	0.96
Common-differential-mode	0.81	0.82	0.93	0.94

VI. CONCLUSION

A novel noise analysis method of radiated EMI is proposed based on NLPCA algorithm in the paper, by separating the mixed radiated noises with NLPCA algorithm, the sources of radiated noise can be found quickly. Then, three groups verification experiments are carried out to verify the effectiveness of NLPCA algorithm in separating noises, the results show that NLPCA algorithm can successfully separate radiated noise from multiple radiated sources. In addition, it can be seen that the accuracy of NLPCA algorithm is higher than ICA algorithm, which improves the accuracy and the efficiency of the radiated EMI noises separation.

ACKNOWLEDGMENT

This paper is sponsored by National Natural Science Foundation of China (51475246), Aviation Science Foundation (20172552017).

REFERENCES

- [1] A. Mueed, Y. Zhao, and Y. Wei, "Analysis of lossy multiconductor transmission lines (MTL) using adaptive cross approximation (ACA)," *Applied Computational Electromagnetics Society Journal*, vol. 34, no. 11, pp. 1769-1776, 2019.
- [2] Y. Zhao and K. Y. See, "A practical approach to EMC education at the undergraduate level," *IEEE Transactions on Education*, vol. 47, no. 4, pp. 425-429, 2004.
- [3] W. Yan, Q. Liu, and C. Zhu, "Semi-inverse method to the Klein-Gordon equation with quadratic nonlinearity," *Applied Computational Electromagnetics Society Journal*, vol. 33, no. 8, pp. 842-846, 2018.
- [4] X. Tong, D. W. P. Thomas, and A. Nothofer, "Modeling electromagnetic emissions from printed circuit boards in closed environments using equivalent dipoles," *IEEE Transactions on Electro-*
- [5] P. Li and L. J. Jiang, "A rigorous approach for the radiated emission characterization based on the spherical magnetic field scanning," *IEEE Transactions on Electromagnetic Compatibility*, vol. 56, no. 3, pp. 683-690, 2014.
- [6] H. H. Park, H. B. Park, and H. S. Lee, "A simple method of estimating the radiated emission from a cable attached to a mobile device," *IEEE Transactions on Electromagnetic Compatibility*, vol. 55, no. 2, pp. 257-264, 2013.
- [7] S. Shinde, X. Gao, and K. Masuda, "Modeling EMI due to display signals in a TV," *IEEE Transactions on Electromagnetic Compatibility*, vol. 58, no. 1, pp. 85-94, 2016.
- [8] A. Nejadpak, A. Sarikhani, and O. A. Mohammed, "Analysis of radiated EMI and noise propagation in three-phase inverter system operating under different switching patterns," *IEEE Transactions on Magnetics*, vol. 49, no. 5, pp. 2213-2216, 2013.
- [9] W. Yan, Q. Tang, and E. Wang, "Radiated emission mechanism for semi-active control strategy of magneto-rheological damper," *International Journal of Applied Electromagnetics and Mechanics*, vol. 51, no. 2, pp. 185-198, 2016.
- [10] S. S. Moghaddam, "Modeling the environmental effects on the radiated fields of a passive RFID system," *International Journal of Applied Electromagnetics and Mechanics*, vol. 42, no. 4, pp. 539-559, 2013.
- [11] S. Jeong, K. Kwak, and G. Park, "A proposed terminal-ground EMI filter for reduction of conducted emissions considering cable radiation and safety," *IEEE Transactions on Electromagnetic Compatibility*, vol. 61, no. 6, pp. 1926-1934, 2019.
- [12] H. C. Hsieh, C. N. Chiu, and C. H. Wang, "A new approach for fast analysis of spurious emissions from RF/microwave circuits," *IEEE Transactions on Electromagnetic Compatibility*, vol. 51, no. 3, pp. 631-638, 2009.
- [13] G. F. Ricciardi and W. L. Stutzman, "A near-field to far-field transformation for spheroidal geometry utilizing an eigen function expansion," *IEEE Transactions on Antennas and Propagation*, vol. 52, no. 12, pp. 3337-3349, 2004.
- [14] B. Ravelo, Y. Liu, and A. K. Jastrzebski, "PCB near-field transient emission time-domain model," *IEEE Transactions on Electromagnetic Compatibility*, vol. 57, no. 6, pp. 1320-1328, 2015.
- [15] B. Zhu, D. J. Chen, and W. Zhong, "A hybrid finite-element/finite-difference method with implicit-explicit time stepping scheme for Maxwell's equations," *In 2011 IEEE International Conference on Microwave Technology and Computational*

Electromagnetics, pp. 481-484, May 2011.

- [16] D. Lin and F. Labeau, "Accelerated genetic algorithm for bandwidth allocation in view of EMI for wireless healthcare," *In 2012 IEEE Wireless Communications and Networking Conference (WCNC)*, pp. 3312-3317, Apr. 2012.
- [17] R. G. Arnaudov and L. G. Plavskiy, "Study of microwave electromagnetic radiation in multilayer QFN package," *In 2010 IEEE 10th International Conference on Actual Problems of Electronic Instrument Engineering (APEIE-2010)*, pp. 130-135, Sep. 2010.
- [18] S. Wang, "Modeling and design of EMI noise separators for multiphase power electronics systems," *IEEE Transactions on Power Electronics*, vol. 26, no. 11, pp. 3163-3173, 2011.
- [19] S. Wang, F. Luo, and F. C. Lee, "Characterization and design of three-phase EMI noise separators for three-phase power electronics systems," *IEEE Transactions on Power Electronics*, vol. 26, no. 9, pp. 2426-2438, 2011.
- [20] S. Wang, Y. Y. Maillet, and F. Wang, "Investigation of hybrid EMI filter s for common-mode EMI suppression in a motor drive system," *IEEE Transactions on Power Electronics*, vol. 25, no. 4, pp. 1034-1045, 2010.



Zhibo Zhu received his B.S. degree in Automation from Nanjing University of Information Science and Technology, Nanjing, China, in 2017. He is currently working in Electromagnetic Compatibility and Power Electronics Devices with Nanjing Normal University. His

interest is the design of Electromagnetic Compatibility of chips.



Wei Yan received his Electrical Engineering M.Sc. and Physics and Electronics Ph.D. degrees from Nanjing Normal University, Nanjing, China, in 2011, and 2014, respectively. Since 2014, he has been with Nanjing Normal University, where he is currently an Associate Professor. His research interests include integrated circuit electromagnetic compatibility testing, and electromagnetic compatibility design, etc.



Yongan Wang received the B.S. degree in Electrical Engineering and Automation from Huaiyin Institute of Technology, Huaian, China, in 2018. He is currently working toward the Master's degree in Electrical Engineering at Nanjing Normal University, Nanjing, China.

His major is electromagnetic compatibility analysis.



Yang Zhao received his B.S., M.Sc., and Ph.D. degrees all in Power Electronic Technology from Nanjing University of Aeronautics and Astronautics, Nanjing, China, in 1989 and 1992, and 1995, respectively. Since 2002, he has been with Nanjing Normal University, where

he is currently the Professor. His research interests are in the areas of Electromagnetic Compatibility, Power Electronics and Automotive Electronics.